**Proceedings of the XVIII ECSMGE 2024**
GEOTECHNICAL ENGINEERING CHALLENGES
TO MEET CURRENT AND EMERGING NEEDS OF SOCIETY

ISBN 978-1-032-54816-6
DOI 10.1201/9781003431749-144


# Combined pile-raft and raft foundation modelling and design for three distinct office buildings in Lisbon, Portugal

## Modélisation et conception combinées de fondations sur pieux et sur radiers pour trois différents immeubles de bureaux à Lisbonne, au Portugal

A. Sousa*, A. Pinto, N. Silva
*JETsj Geotecnia, Lisbon, Portugal*
**asousa@jetsj.com*

**ABSTRACT**: In recent years many projects were designed using the Combined Pile-Raft Foundation (CPRF) concept. Combined Pile-Raft Foundations have a complex soil-structure interaction scheme including the pile-soil interaction, pile-pile interaction, raft-soil interaction, and finally the pile-raft interaction. Consequently, there is a need for 3D numerical models that can study this complex interaction. In this paper, several 3D models are presented and discussed for the foundation design of three office buildings, that were built using the Combined Pile-Raft and Raft Foundations solutions, near the right bank of the Tagus River in Lisbon, Portugal. The study was based on geotechnical information provided by the site investigation and by Static and Dynamic Load Tests on Driven Piles, both performed in several spots evenly distributed at the site. The developed 3D model was able to simulate the behaviour of the piled raft foundation system.

**RÉSUMÉ**: Ces dernières années, de nombreux projets ont été conçus en utilisant le concept de fondation combinée sur pieux et radeau. Les fondations combinées pieux-radeau ont un schéma d'interaction sol-structure complexe comprenant l'interaction pieu-sol, l'interaction pieu-pieu, l'interaction radeau-sol et enfin l'interaction pieu-radeau. Par conséquent, il existe un besoin de modèles numériques 3D capables d'étudier cette interaction complexe. Dans cet article, plusieurs modèles 3D sont présentés et discutés pour la conception des fondations de trois immeubles de bureaux, qui ont été construits à l'aide des solutions de fondations combinées Pile-Raft et Raft, près de la rive droite du Tage à Lisbonne, au Portugal. L'étude s'est basée sur les informations géotechniques fournies par l'investigation du site et par des essais de charge statique et dynamique sur pieux battus, tous deux effectués à plusieurs endroits uniformément répartis sur le site. Le modèle 3D développé a pu simuler le comportement du système de fondation sur radiers sur pieux.

**Keywords:** 3D modelling; raft foundation; combined pile-raft foundation; finite element method.

## 1 INTRODUCTION

The use of piles, strategically located, within a raft foundation has been a commonly accepted practice, which has been used in many projects, to improve both the ultimate load capacity and the settlement and differential settlement performance of the raft.

This paper presents the modelling and geotechnical design of pile-raft and raft foundation solutions for three office buildings built close to the Tagus River, in Lisbon, Portugal (Figure 1). The proximity to the river brought geological and geotechnical restraints that will be further discussed and analysed in the next sections.

The three lots had different constraints regarding the number of basements, and the total number of stories as shown in Table 1:

*Table 1. Geometry information table on the 3 lots.*

| Designation | Area (m2) | Stories | Basements | Excavation Depth (m) |
|---|---|---|---|---|
| Lot 1 | 2000 | 12 | 3 | 11 |
| Lot 2 | 6350 | 9 | 2 | 6 |
| Lot 3 | 5000 | 8 | 2 | 7 |

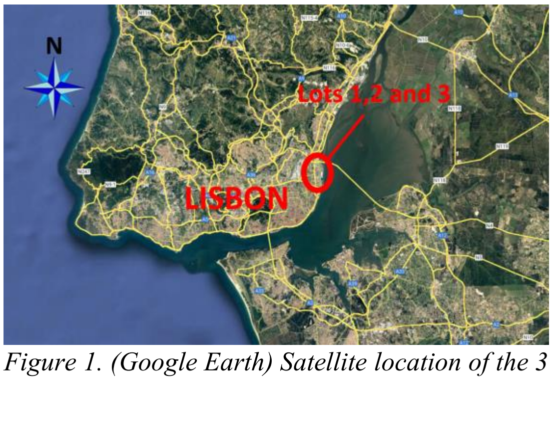


*Figure 1. (Google Earth) Satellite location of the 3 lots.*

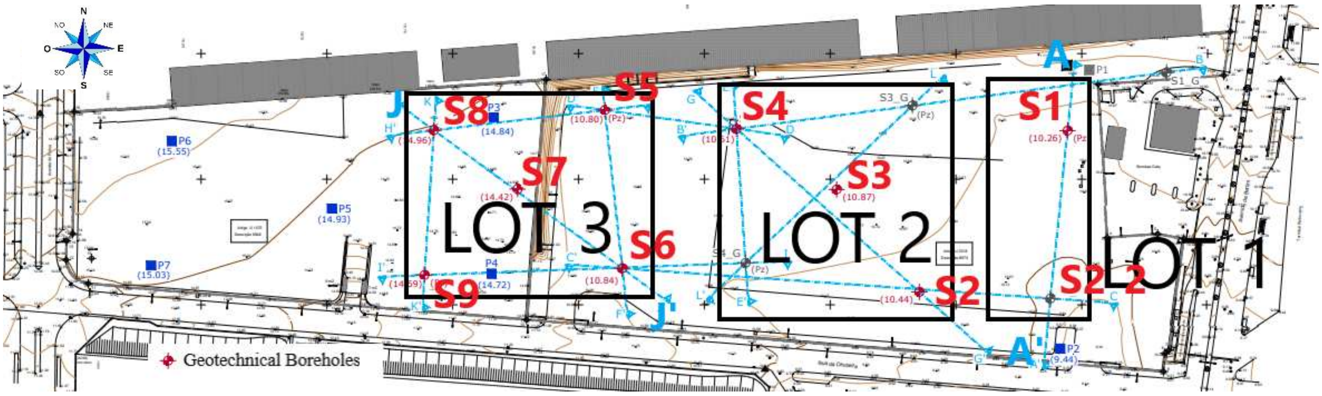


*Figure 2. Building lots and boreholes for geotechnical investigation.*

## 2 GEOTECHNICAL CONSTRAINTS

This section presents the main geotechnical constraints that affected the solutions studied.

### 2.1 Geotechnical investigation

A site investigation campaign consisting of eleven boreholes was conducted with SPT tests. The location of the boreholes is shown in Figure 2.

In general, the area where the lots are located is at a low topography level in an alluvial zone, corresponding to old water courses that formerly flowed into the Tagus River, with a general orientation WNW-ESE (main water course) and SW-NE (secondary water course). Under these alluvial deposits layer is the Miocene layer, characterized by the "Areolas de Braço de Prata" which is formed by dense sands and clays (as illustrated in Figure 3 Figure 4).

Throughout the area landfill deposits were identified, resulting from various anthropic actions developed over time and of diverse nature.

Table 2 shows the several layers detected in the investigation campaign, along with the SPT test results.

*Table 2. Prospected layers by the investigation campaign.*

| Geotechnical Zone | Lithology | NSPT |
|---|---|---|
| ZG1 | Landfill and other materials that may have been displaced | 1-17 |
| | Alluvial Deposits | 0-8 |
| ZG2A | Fine silty-clayey sands and sandy silts | 10-41 |
| ZG2B | Silty clays, clayey silts and sandy silts | 24-60 |
| ZG2C | Fossiliferous lumachelic/calcarenite levels | >60 |

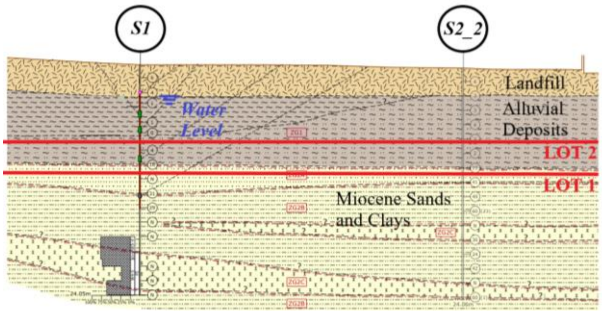


*Figure 3. Site investigation geotechnical profile (Section Cut AA' from S1 to S2_2 at lot 1).*

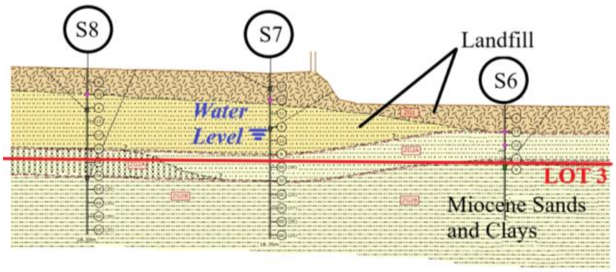


*Figure 4. Site investigation geotechnical profile (Section Cut JJ' from S8 to S6 at lot 3).*

### 2.2 Hydrology and permeability

The study of the ground permeability, as well as of the water lines crossing the site area, proved to be particularly important for the design and execution of the foundation solutions.

These permeabilities were evaluated based on laboratory analyses of samples taken during the boreholes drilling.

The Miocene layers in the investigated area are composed of fine silty-clayey sands, sandy silts, and silty clays, sometimes with the intercalation of very fossiliferous levels. In general, this Miocene complex has porosity permeability (primary), but locally it may present fissure permeability in the more carbonate/fossiliferous layers (secondary permeability).

This Miocene complex, due to its fine sandy, silty-sandy, and clayey-sandy composition, has overall moderate to low permeability, providing unfavourable conditions for water percolation, with moderate to not significant flows. The retaining walls for the excavation of all lots reached this layer with lower permeabilities, which drastically reduced the water inflow into the excavation pits. In general, the foundations for the three lots were several meters below the investigated ground water level.

## 3 FOUNDATION SOLUTIONS

Two types of foundation solutions were adopted for the three lots.

The main criteria for choosing the solution was the control of differential settlements. In cases where the foundation level was directly over the more dense Miocene layer, a raft solution was recommended. When the foundation level intersected alluvial deposits, a combined pile-raft foundation solution (CPRF) was studied to control deformations.

### 3.1 Raft foundation

The raft foundation solution consists of a continuous slab, connected to the retaining walls by bolts. In the areas where there are higher loads, as for example under the lifts and stairs boxes, greater thicknesses were considered in order to better control differential settlements.

This type of solution allows the hydrostatic vertical uplift pressures, which can be mobilized in the long term, to be accommodated, without having to provide an extensive drainage solution.

### 3.2 Combined pile-raft foundation

The combined pile-raft foundation (CPRF) consists of a raft foundation (as described before) with soil inclusions in areas with greater concentration of loads. In this case, rectangular barrettes were considered, using the same diaphragm wall technology used for the execution of the retaining walls. At areas under structural columns, thicker areas of the slab were adopted, with driven precast piles resting over the more dense Miocene layer (Miocene sands and clays), in order to reduce settlement in these areas and to homogenise displacements throughout the foundation (Figure 5).

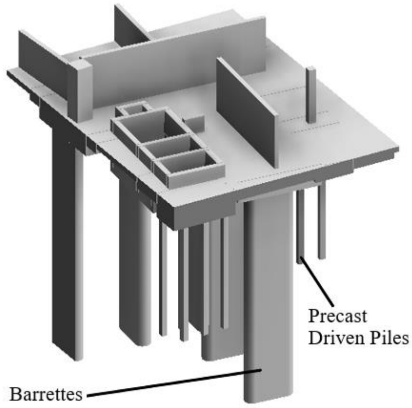


*Figure 5. Pile-raft foundation solution at lot 2.*

## 4 STRUCUTRAL DESIGN

### 4.1 Raft foundation design

The design of a raft foundation consists of the distribution of the loads that come from the structure to the slab, which in turn will transmit them to the ground.

The key issue to this type of design is to minimise the differential settlements derived from the heterogeneous spatial distribution of structural loads.

In this particular case, there is also the action of uplift hydrostatic pressures, which were taken into account in the long-term design of this slab.

To reduce the differential settlements, thicker areas of the foundation slab were adopted under the structural columns and walls.

The design of raft foundation solutions considered the following main design states:

- Maximum total settlements;
- Differential settlements;
- Bending moments and shear forces at the raft.

### 4.2 Combined pile-raft foundation design

There are several design methods for combined piled-raft foundations, with guidelines from Poulos (2000, 2001), Poulos et al. (2011), Fellenius (2015), among others. The main goal is that the load is transferred to the ground by both the raft and piles. The loads are resisted by the bearing capacity between the raft and soil and by the lateral friction and end bearing capacity of the piles. The design method should comprise 4 phases:

- Preliminary study where the viability of the solution is analysed;
- Mapping of the piles and definition of their general characteristics;
- Detailed study of the optimal number of piles;

- Estimation of settlements, bending moments, and shear forces at the raft, as well as axial loads and bending moments at the piles.

The design of CPRF solutions considers, according to Poulos (2001):

- Ultimate bearing load for axial, shear stresses, and bending moments;
- Maximum total settlement;
- Differential settlement;
- Bending moments and shear forces at the raft;
- Bending moment and axial loads at the piles.

## 5 IN SITU TESTS – PDA

To estimate the real bearing capacity of the precast driven piles, 9 load dynamic load tests were performed using the "Pile Driving Analyser (PDA)" method. The tests were performed on a square prefabricated reinforced concrete piles of section 300x300mm2 (Figure 6).

The results obtained from the dynamic load test indicate several layers of low to medium strength up to a depth of approximately 2.9 to 13.1 m, where the shaft resistance is lower than 90 kPa. Under this layer, a zone of higher resistance was found, with a shaft resistance ranging from 128 to 524 kPa. The tip resistance for these piles was between 14.6 and 18.2 MPa.

These values (both for the shaft and tip resistance) are an underestimation since low energy was being transferred during these tests to guarantee pile integrity.

*Figure 6. Pile Driving Analyser preliminary tests being executed at lot 2.*

## 6 MODELLING

The modelling was performed using software PLAXIS 3D. For the pile-raft foundation of lot 2, PLAXIS 2D axisymmetric analysis were also used for the calibration of the modelled inclusions with empirical methods widely used in the past.

### 6.1 FE models for structural elements

Different finite element (FE) models were chosen for each of the structural elements to simulate their behaviour in both the short and long term.

#### 6.1.1 Foundations *slabs*

The foundation slabs were modelled with plate elements (PLAXIS, 2023).

#### 6.1.2 Precast driven piles and barrettes

Both the precast driven piles and the barrettes were simulated using the embedded beam element in PLAXIS 3D. These elements describe the interaction between the piles and the surrounding soil. The interaction at the shaft and at the tip is described by means of embedded interface elements. The pile is considered as a beam which can cross a volume element at any place with any arbitrary orientation. Due to the existence of the beam element three extra nodes are introduced inside the volume element.

#### 6.1.3 Connection between the foundation slab and the retaining wall

The retaining wall and the foundation slab are connected by a linear element which allows shear forces to be transmitted, however rotations are free. This behaviour allows the simulation of the bolted connection between the two elements.

#### 6.1.4 Structural columns and walls

The structural loads for all relevant combinations, are simulated in the model by means of point loads applied at the gravity centre of the structural columns and walls.

The structural wall behaviour was simulated by implementing a rigid beam along the wall centreline, which will redistribute the point load along the walls path, and therefore avoiding any numerical problems that may appear due to the high concentrated loads (applied at the walls gravity centres).

#### 6.1.5 Soil elements

The soil was modelled using the hardening soil model, with volume elements in the 3D models. The Miocene sand layers were set to respond with a drained behaviour and the Alluvial deposits, and the Miocene clay layers were set to respond with an undrained behaviour (effective stress analysis) (Table 3, Table 4 and Table 5).

Both short term and long-term situations were accounted for in the analysis.

*Table 3. Material models adopted in the 3D Model.*

| | Properties | |
|---|---|---|
| | **Material model** | **Drainage type** |
| ZG1 | HS | Undrained (A*) |
| ZG2A | HS | Drained |
| ZG2B | HS | Undrained (A*) |
| ZG2C | HS | Undrained (A*) |

**Undrained calculations were performed using effective stress properties. Long-term behaviour was also considered in the model.*

*Table 4. Material stiffness in the 3D Model.*

| | Stiffness | | |
|---|---|---|---|
| | **$E_{50}^{ref}$ (kPa)** | **$E_{oed}^{ref}$ (kPa)** | **$E_{ur}^{ref}$(kPa)** |
| ZG1 | 10000 | 10000 | 30000 |
| ZG2A | 50000 | 50000 | 150000 |
| ZG2B | 100000 | 100000 | 300000 |
| ZG2C | 150000 | 150000 | 450000 |

*Table 5. Material strength parameters in the 3D Model.*

| | Resistance | |
|---|---|---|
| | **$c'^{ref}$ (kPa)** | **φ' (º)** |
| ZG1 | 1 | 28 |
| ZG2A | 1 | 38 |
| ZG2B | 40 | 36 |
| ZG2C | 20 | 39 |

#### 6.1.6 PLAXIS 2D axisymmetric modelling for embedded beam behaviour calibration

The three-dimensional model for lot 2 was calibrated using the axisymmetric mode of PLAXIS 2D, where the response of the embedded beams was compared with the real pile behaviour.

The results (illustrated on Figure 7) show that the loads, for the failure criterion, estimated using the 2D axisymmetric model match the maximum service load calculated using empirical methods (Bustamante and Gianeselli, 1993, 1998).

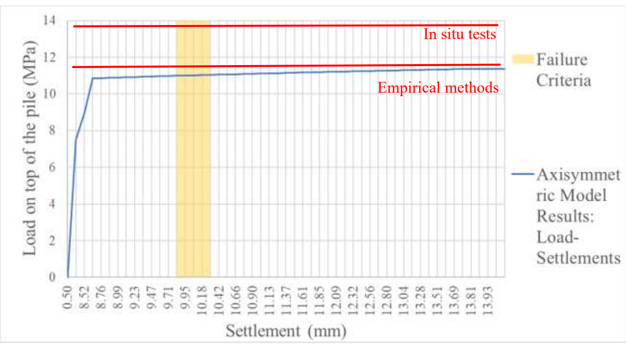


*Figure 7. Load-Settlement obtained in the 2D model.*

An ultimate load of 990kN was obtained for the failure criteria, for the precast driven piles.

These results were lower than the values obtained in the PDA tests. This shows that the empirical methods used, that are based on a collection of data from numerous field trials, take on assumptions so that the calculated values (using the methods) for the bearing capacity are, in most cases, conservative in relation to their actual capacity.

## 7 FINAL DESIGN

For the safety verification against relevant limit states, partial safety factors relative to both the actions and the materials, were adopted according to the European standard regulations.

### 7.1 Ultimate limit states

The final design of the foundation slab and the deep foundation elements was made using the results of the three-dimensional models, duly calibrated.

A load envelope was considered for each structural element, based on the most relevant combinations.

It should be noted that the lots in question are located in a seismic zone, and therefore there are, in all the buildings, sets of stairs and lift boxes and walls that have severe loads that need to be transmitted to the foundations.

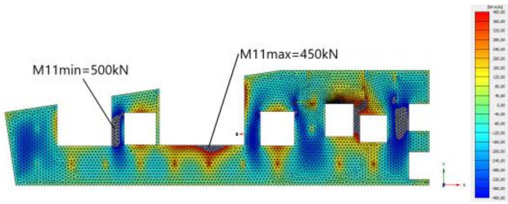


*Figure 8. Bending moments M11 at the raft plate for a single combination in the lot 1 model.*

Figure 8 shows the distribution of the bending moments in the lowest thickness slab. The distribution of loads on the slab leads to cylindrical bending between the spans without deep foundation elements. The areas over deep foundations will be stiffer, and therefore behave as supports for the hydrostatic uplift pressures.

Both solutions were designed against punching. It's crucial to thoroughly assess the hydrostatic uplift pressures exerted on the bottom of the foundations in these types of solutions, especially considering that the column loading acts in a different direction.

All the precast driven piles and the barrettes were checked for combined axial force and biaxial bending, adopting the results from the model (Figure 9).

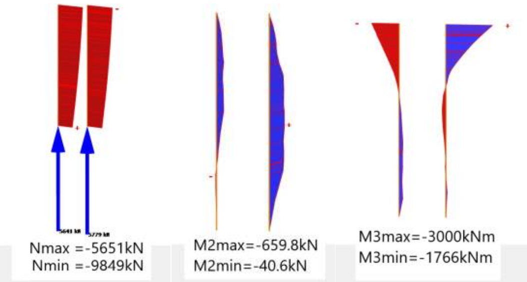


*Figure 9. Forces in a pair of barrettes, modelled as embedded beams, for a single combination at lot 2.*

## 7.2 Service limit states

### 7.2.1 Verification of the maximum settlements

The maximum settlement for each model was accessed and checked, for the relevant combinations. The maximum values of 6.7 mm, 20.3 mm and 16.3 mm were obtained, respectively, for lots 1, 2 and 3.

### 7.2.2 Verification of differential settlements

To check the differential settlements, the maximum rotations over two points in the foundations system were estimated for each model.

Equation (1) shows the formula used to check the rotations at lot 1.

$$\tan\left(\theta_{rel,max}\right) = \tan\left(\frac{(\delta_{max}-\delta_{min})\times 10^{-3}}{distance}\right) = \tan\left(\frac{(6.7-2)\times 10^{-3}}{15}\right) = 5.5\times 10^{-5} \leq \frac{1}{2000} = 5\times 10^{-4} \quad (1)$$

where $\theta_{rel,max}$ is the rotation (angle) between two points with the settlements $\delta_{max}$ and $\delta_{min}$

### 7.2.3 Verification of the global settlements near the façade, due to architectural limitations

Due to architectural constraints, it was necessary to verify the differential settlements at the lots peripherical zones. The models provided the ability to quickly access this information, as shown in Figure 10, for lot 2.

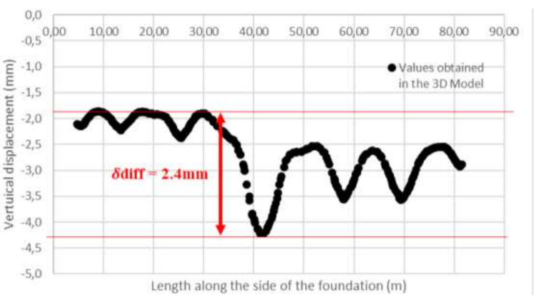


*Figure 10. Long-term total settlements from two corners at the lot 2 model.*

## 8 CONCLUSIONS

Higher processing power and access to smaller and greater data storage units are allowing more complex models to be quickly assembled. The described type of model can now be built, calibrated, and ran within most foundation projects time frame and enables the study of crucial issues in this type of project, such as soil-structure interaction, soil permeability, different settlements caused by different foundation stiffness zones, geological and geotechnical changes throughout the area site and much more, to be simulated effectively, henceforth allowing for optimized foundation solutions.

## ACKNOWLEDGEMENTS

The authors would like to thank the Contractor “HCI construções” and the owner “EXPO ATLÂNTICO, EPII INVESTIMENTOS IMOBILIARIOS S.A. “for authorising the writing and presentation of this article.

## REFERENCES

Bustamante, M. and Gianeselli, L. (1993). Design of auger displacement piles from in situ tests. *Deep Foundations on Bored Auger Piles, BAP II*, Balkema, Rotterdam, 21-34. https://doi.org/10.1201/9781003078517-12.

Bustamante, M. and Gianeselli, L. (1998). Installation parameters and capacity of screwed piles. *Deep Foundations on Bored Auger Piles, BAP III*, Balkema, Rotterdam, 95-108.

Fellenius, B. H. (2015). *Basics of foundation design (Revised IE)*. Retrieved from www.Fellenius.net.

PLAXIS bv. (2023). PLAXIS 3D Version 2023.1, *Reference Manual*. Delft, The Netherlands. https://doi.org/10.1155/2023/6693876.

Poulos, H. G. (2000). Practical Design Procedures for Piled Raft Foundations. In J. Hemsley, *Design Applications of Raft Foundations,* 425-467. London: ICE Publishing. https://doi.org/10.1680/daorf.27657.0016.

Poulos, H. G. (2001). *Piled Raft Foundations: Design and Applications. Geotechnique*, 51(2), 95-113.

Poulos, H. G., Small, J. C., Chow, H. (2011). Piled Raft Foundations for Tall Buildings. *Geotechnical Engineering Journal of the SEAGS and AGSSEA*, 42(2), 78-84.